

Response to Reviewer #1

Dear Reviewer,

Thank you for the time and effort you have dedicated in providing valuable feedback on the manuscript. We have been able to incorporate most of the suggestions provided. The manuscript has clearly benefitted from the review process, and we hope you also find that the suggestions have made our manuscript suitable to publication. All authors agree with the modifications made to the manuscript. The comments by the referee are reported in italic font followed by our response. The line numbers reported in the answers referred to the location in the revised manuscript. The new supplementary figures are also provided at the end of this document.

Major Comments:

The definition of upwelling, non-upwelling, and oceanic locations is indeed interesting, but it does not look very statistically robust. Are these locations constant in time? If you calculate the correlations for different periods, are the locations the same? This a very important potential issue that should be addressed.

We understand your concern about the statistical robustness of our location. In order to address this issue, we performed two analyses. The first analysis is similar to the one used in (Barton et al., 2013) to build confidence in the trend. The figure beneath shows how in sub-series shorter than 15 years (30 years) in the case of the northern (southern) hemisphere's EBUS trends varied widely. However, we found that with sufficiently long time series, the upwelling cell trends stabilized and became independent of the period. The confidence intervals reveal statistical significance at 90% in all the major upwelling cells used in this study (exact values of the trend will be added in figure 4).

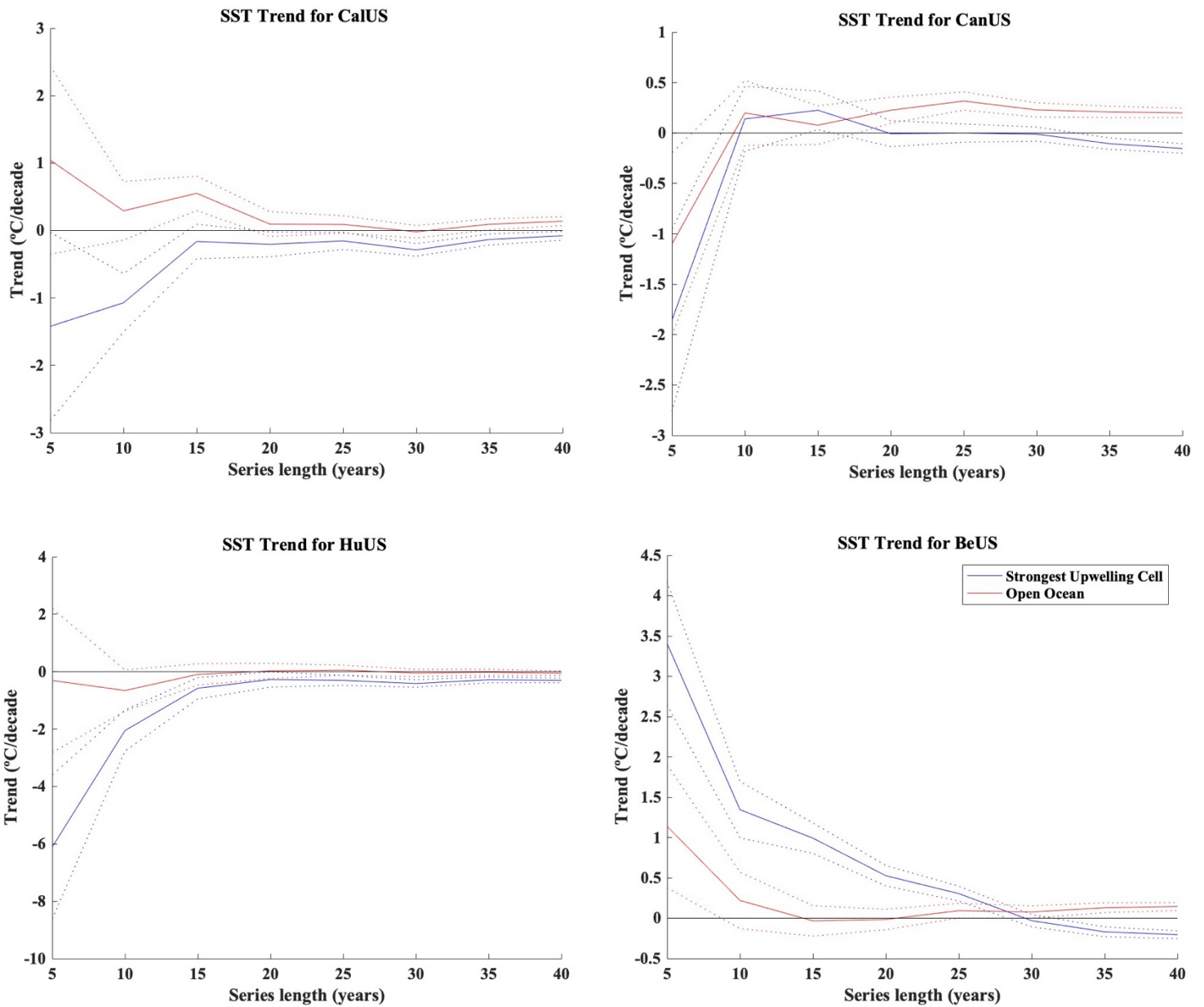
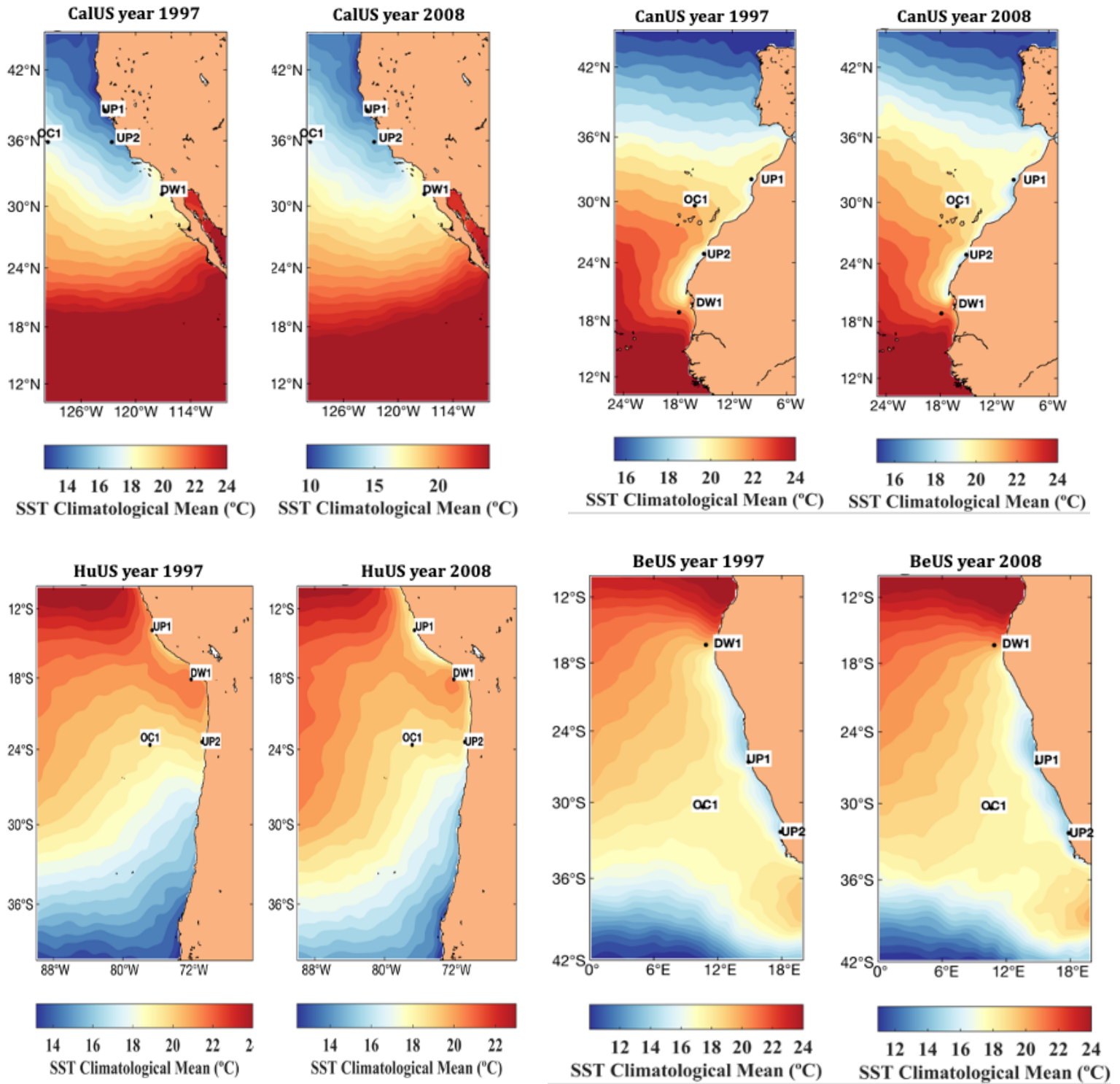


Fig S5: Trend values calculated as a function of series length for SST trends in the higher upwelling cell and open ocean areas. Trend values are shown as solid lines and 90% confidence limits as broken lines.

The second analysis performed consisted in analyzing the SST field to account for the spatial stability of the location. Thus, we examined the mean field in anomalous years, when the variability of the upwelling center should be maximum, like El Niño and La Niña years (1997 and 2008, respectively, see figure beneath). For both cases the locations of the upwelling centers are the same even in El Niño years, although the extension of the upwelling center may vary.



Mean SST fields comparison for El Niño (1997) and La Niña (2008) year in each EBUS.

In addition, and attending to a comment of reviewer #2 we analyzed the change in the angle due to changes in the latitude of the upwelling center, and it suggests that the points are representative of the permanent upwellings. Beneath the new Figure Fig 6 added on the manuscript.

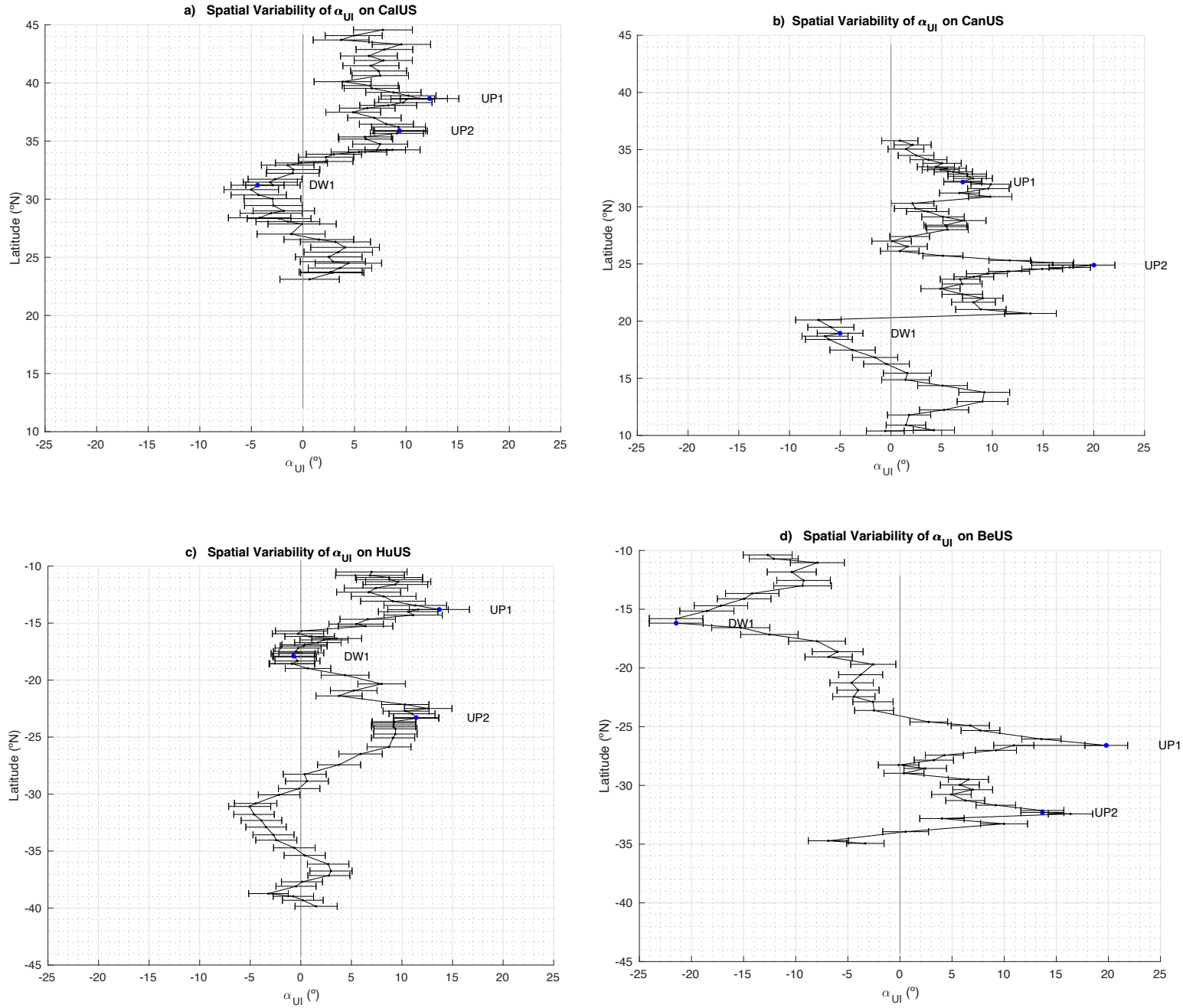


Fig 6: Spatial distribution of the α_{UI} (over the period of 1982-2021) along the coast for CalUS (a), CanUS (b), HuUS(c) and BeUS(c). The α_{UI} is calculated between grid points along the coast and OC1, with error bars representing the Monte Carlo error for each grid point. Key locations UP1, UP2, and DW1 are highlighted with blue markers.

You say that analyzing the upwelling locations is better than using spatially-averaged regions, you also discuss other papers, but what about your own results for averaged regions? You should contrast your current results to larger averaged regions. And

remember, one advantage (a very important indeed) is that the spatial average should reduce errors.

Thank you for your suggestions. We agree with the reviewer on the importance of providing additional information regarding the effects of averaged regions on our results. While spatial averaging can reduce errors, it is crucial to focus on upwelling regions to fully capture the main dynamical processes. To address this issue, we used four different averaging zones in our study. Zone A, encompassed a large average of the whole coastal region. Zone B, covered an area just large enough to include the three main coastal upwelling areas (UP1, UP2 and DW1). Zone C, focused around the two main upwelling centers of each region, and Zone D, targeted only the strongest upwelling center. The results are summarized in the following table:

Zone	CalUS	CanUS	HuUS	BeUS
A	2°±2°	2°±2°	3°±2°	1°±2°
B	3°±2°	2°±2°	4°±2°	2°±2°
C	8°±3°	7°±2°	9°±2°	9°±2°
D	10°±3°	15°±2°	12°±3°	16°±2°
This Study	11°±3°	20°±2°	14°±3°	21°±2°

Table S1: α_{UI} estimation for different portions of the coastal region: the whole coastal area, Zone A, covered an area just large enough to include the three main coastal upwelling areas (UP1, UP2 and DW1), Zone B, focused around the two main upwelling centers of each region, and Zone C, and targeted only the strongest upwelling center, Zone D. Last Row show the results obtained in figure 5.

When we averaged over larger regions, ignoring the specific dynamics of the upwelling zones, our results remained consistent regardless of the area size. This suggests that larger spatial averaging does indeed reduce random errors. However,

this approach tends to obscure the finer-scale dynamics and local variations that are critical for understanding upwelling processes.

In contrast, when we focused on specific upwelling zones, selecting the areas around upwelling centers (Zones C and D), our results were very similar to those obtained without averaging areas. This indicates that focusing on precise upwelling locations captures the essential features of the upwelling dynamics, providing results that are both accurate and representative of the localized processes. Based on these results, we have decided to add these results to the discussion in line 442 as follow:

‘...Additionally, we tested the effects of averaging areas around the upwelling cells to build the index (see supplementary material, Fig S5). We compare the results obtains in this manuscript with the index recalculated for different average portions of the coastal regions in each EBUS. First, we computed the index for the entire coastal region, referred to as zone A in the supplementary material. The results in zone A remained positive although the mix of the different dynamical regions in each area resulted in non-significant values. Similarly, zone B is a large average region but covering only the three different dynamical areas in this study. Again, the results were positive but not significant when using large averaged portions of the coastal regions. In contrast, focusing on the surrounding of upwelling zones (zone C which includes both upwelling center, UP1 and UP2, and zone D, which includes only the surroundings of the main upwelling center), made the intensification more evident, especially in zone D where results are the closest values compare to the results in this manuscript. Moreover, we verified the stability of the trends both spatially and temporally by performing the analysis of Barton et al. (2013) across all EBUS (see supplementary material Fig S5)’.

What about the significance test for the trends? Some trend values seem to be too small their values should be shown to be significant.

The 90% confidence is added to figure 4 for reliability.

Table 1: Plots of satellite-data comparisons should be included; Table 1 should be a complement for these plots.

Thank you for your suggestion. We agree that the comparison is relevant for the study and that it is necessary to support the tables with plots of satellite data

comparison. However, they will be added to supplementary information for the sake of text clarity.

The proposed index is potentially useful, but it does not provide a convincing argument to confirm the Bakun hypothesis. The analysis of an additional variable, for example sea-level pressure, could be useful to confirm such a hypothesis. Other explanations for the upwelling (e.g., Arellano and Rivas, 2019).

This is a fair point. While SST is useful and reliable for inferring upwelling intensification, it does not provide enough information about its drivers. To address this, we analyzed the trends in pressure gradients from 1982 to 2023 using two well-known datasets: ERA5 and NCEP, to complement our findings on the α_{UI} .

For ERA5, we found positive and significant trends (see table beneath) for all EBUS. Although small, these trends are all significant. On the other hand, the NCEP dataset shows no significant trend for the BeUS but stronger trends than ERA5 for the other EBUS. However, due to its coarser resolution (2.5°) compared to ERA5 (1/4°), NCEP data is arguably less reliable. Nevertheless, these results support an intensification of the pressure gradient, aligning with Bakun’s hypothesis of enhanced upwelling-favorable winds.

	CalUS (mb/decade)	CanUS (mb/decade)	HuUS (mb/decade)	BeUS (mb/decade)
ERA5	0.24 (0.039)	0.04 (0.017)	0.33 (0.038)	0.15 (0.051)
NCEP	0.37 (0.073)	0.17 (0.034)	0.54 (0.070)	-0.02 (0.072)

Table 3. Values of the trend, over the period 1982-2023, for the ERA5 (first row) and NCEP (second row) for all the EBUS. Parentheses enclose spatial standard deviation.

Additionally, as suggested by studies such as Rykaczewski et al. (2015) and Arellano and Rivas (2019), the migration of large-scale pressure systems offers an alternative explanation for upwelling intensification trends. Their research indicates that shifts in pressure systems can significantly impact upwelling regions, influencing wind patterns and subsequently upwelling processes. However, there are still open questions about the nature of the intensification, as a poleward migration of high-pressure systems could also contribute to these trends. Therefore, a new section will be included in line 386 to accommodate the new results:

“4.5. SLP Gradients

The coastal upwelling intensification postulated by Bakun (1990), would involve a stronger increase of near-surface temperature over land than over the ocean, which would lead to an intensification of the continental thermal low-pressure system relative to the ocean. To test this driver mechanism, we have calculated the trends (Fig 7) of the pressure gradient between the continental thermal low and the oceanic high pressure.

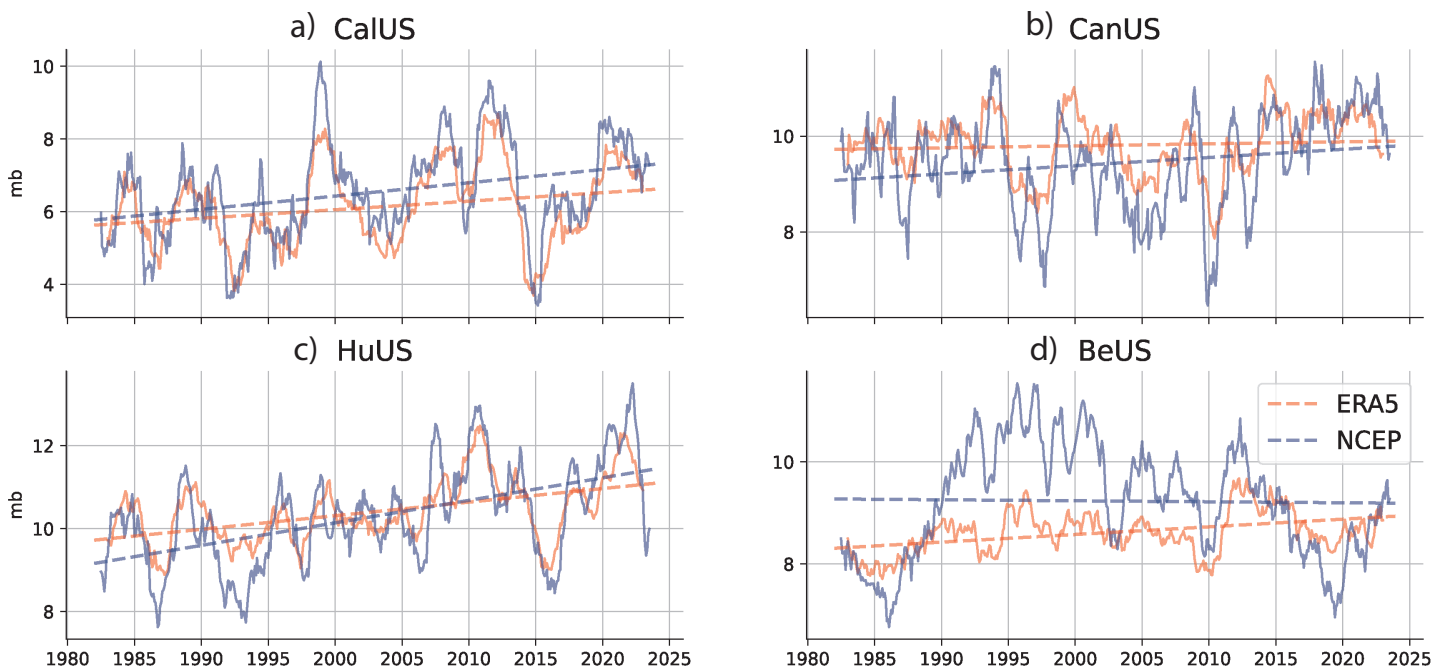


Fig 7: EBUS SLP gradients trends and temporal series for NCEP (blue lines) and ERA5 (red lines) datasets over the period 1982- 2023.

For ERA5, we found positive and significant trends (see Table 3) for all Eastern Boundary Upwelling Systems (EBUS). Specifically, the trends in SLP gradients are 0.24 mb/decade (with a spatial standard deviation of 0.039 mb/decade) for CalUS, 0.04 mb/decade (0.017 mb/decade) for CanUS, 0.33 mb/decade (0.038 mb/decade) for HuUS, and 0.015 mb/decade (0.051 mb/decade) for BeUS. On the other hand, the NCEP dataset shows no significant trend for the BeUS but stronger trends than ERA5 for the other EBUS, with 0.37 mb/decade (0.073 mb/decade) for CalUS, 0.17 mb/decade (0.034 mb/decade) for CanUS, 0.54 mb/decade (0.070 mb/decade) for

HuUS, and -0.02 mb/decade (0.072 mb/decade) for BeUS. However, due to its coarser resolution (2.5°) compared to ERA5 (0.25°), NCEP data is arguably less reliable.”

In Section 5 we have included the following discussion in line 543:

“The SST changes in the EBUS respond mainly to changes in the upwelling processes which are ultimately driven by the pressure gradients. We analyzed the pressure gradients trends in all four EBUS. Our findings further support the intensification of the pressure gradients driven by climate change, as stated by (Bakun, 1990). However, there are probably other contributors to the intensification of the upwellings. Some researchers question whether the impacts of differential heating on the pressure gradient force drives intensification of coastal upwelling. Rather, a complementary hypothesis proposes that evidence of an intensifying pressure gradient force is limited to poleward migration of the Hadley Cell (Arellano & Rivas, 2019; Rykaczewski et al., 2015; Wang et al., 2015). Nevertheless, these projections are only supported by observational records in the Humboldt and Benguela Systems, (Sydeman et al., 2014). In contrast, we have tested this hypothesis on the historical record by computing the latitudinal distribution of α_{UI} . The results shown in Fig 6 partially agree with Rykaczewski et al, (2015), as only CalUS and BeUS presented a poleward intensification of α_{UI} . To further understand the drivers of these changes, we examined the spatial stability of the trends in the SLP continental-oceanic gradient was also tested using Monte Carlo simulation. The discrepancy between the latitudinal distribution of α_{UI} and the small standard deviation of trends around the cores of the pressure systems suggests that the hypothesis of poleward displacement of the high-pressure systems remains inconclusive.’

Minor Comments:

Methods: You could include the historical hydrographic data available at NOAA – World Ocean Database (WOD).

Thank you for your suggestion. The SST data set that we have used has been calibrated using in-situ observations (Reynolds et al., 2007), and additionally we have used in-situ observations to demonstrate that the data set is representative of the SST in-situ observations. Therefore, we have used all the historical hydrographic data in the area to validate the results.

93: *Specify the period used to calculate the monthly climatology.*

The period will be added in line 158 as: "...NOAA SST analyses data (1982-2021) into..."

119: *"unitary vector normal (n) to", unit vector (n) normal to...*

Thank you for your suggestion, this change will be incorporated to the manuscript.

122: *"atan2" is not a standard notation for the arc tan.*

We thank the reviewer for pointing this out. The notation was made to clarify the lector that we are using the four-quadrant arc tangent which is a function of two arguments that allow identification of the angle sign. However, to respect standard notation we will include the clarification as a footnote as follow in line:

$$\alpha_{UI} = \arctan^* \left(\frac{(\overline{U_p} \times \overline{O_c}) \cdot \overline{n}}{\overline{U_p} \cdot \overline{O_c}} \right) = \arctan \left(\frac{|\overline{U_p}| |\overline{O_c}| \sin(\alpha_{UI})}{|\overline{U_p}| |\overline{O_c}| \cos(\alpha_{UI})} |\overline{n}| \cos(\beta) \right)$$

* We used the four-quadrants arc tangent in this analysis since it allows to determine the sign of the angle based on the signs of the arguments."

134: *What about error propagation?*

Thank you for your comment. We have carried out Monte Carlo simulation as described in section 3.3 which already accounts for the full variability of both temporal series. We will rephrase the text in line 197:

'...We also conducted a probabilistic assessment of uncertainties for α_{UI} , taking into account the uncertainties associated with upwelling and open ocean SST series. We performed error estimation using the Monte Carlo method: residual errors for individual data points were separately and randomly sampled 10,000 times within their respective $\overline{U_p}$ - and $\overline{O_c}$ - uncertainty ranges. These sampled errors were then used to calculate α_{UI} . The standard deviation of the 10,000 simulations represents the uncertainty of α_{UI} .'

137-138: *"...shifts northward in summer", this is not accurate, especially in the southern portion of the upwelling system*

Thank for you comment. The text will be modified as follow: "...CalUS. In summer the strongest winds occur..."

141: *"...and Point Conception", south of it, the wind's seasonal variability is different.*

Thank for you comment. The text will be modified accordingly

Caption of Figure 2: "...buoys", moorings.

Following the reviewer's comment, we have modified Figure 2 caption accordingly

210: *"...this areas", these areas.*

The text will be modified accordingly

Section 4.2 (and rest of the text): Three decimals in the trend values is probably excessive, two should be enough or justify why you use three. Also, for example, a trend of -0.2 °C/decade should be -0.20 °C/decade or, if three decimals are used, -0.200°C/decade; remember, significant decimals.

Following the reviewer's suggestion two decimals will be implemented (using truncation) when possible (e.g. 0.007 °C/decade).

243: *"Luderitz cell", include a reference.*

The following references will be included in section 3.4 and 4.2:

295: *"spikes", peaks. "...Niño appeared...", ...Niño that appeared...*

Thank for your suggestions. "spikes" will be replaced by "peaks"

364: *Define IPO.*

Following reviewer suggestion the definition of IPO will be added in line 515: "the Interdecadal Pacific Oscillation (IPO)"

366-372: *Specify the periods used for the trend calculations in those references.*

Period now are specified in the text

References:

Arellano, B., & Rivas, D. (2019). Coastal upwelling will intensify along the Baja California coast under climate change by mid-21st century: Insights from a GCM-nested physical-NPZD coupled numerical ocean model. *Journal of Marine Systems*, 199, 103207. <https://doi.org/10.1016/J.JMARSYS.2019.103207>

- Bakun, A. (1990). Global climate change and intensification of coastal ocean upwelling. *Science*, 247(4939), 198–201. <https://doi.org/10.1126/science.247.4939.198>
- Barton, E. D., Field, D. B., & Roy, C. (2013). Canary current upwelling: More or less? *Progress in Oceanography*, 116, 167–178. <https://doi.org/10.1016/j.pocean.2013.07.007>
- Reynolds, R. W., Smith, T. M., Liu, C., Chelton, D. B., Casey, K. S., & Schlax, M. G. (2007). Daily high-resolution-blended analyses for sea surface temperature. *Journal of Climate*, 20(22), 5473–5496. <https://doi.org/10.1175/2007JCLI1824.1>
- Rykaczewski, R. R., Dunne, J. P., Sydeman, W. J., García-Reyes, M., Black, B. A., & Bograd, S. J. (2015). Poleward displacement of coastal upwelling-favorable winds in the ocean's eastern boundary currents through the 21st century. *Geophysical Research Letters*, 42(15), 6424–6431. <https://doi.org/10.1002/2015GL064694>
- Sydeman, W. J., García-Reyes, M., Schoeman, D. S., Rykaczewski, R. R., Thompson, S. A., Black, B. A., & Bograd, S. J. (2014). Climate change and wind intensification in coastal upwelling ecosystems. *Science*, 345(6192), 77–80. <https://doi.org/10.1126/science.1251635>
- Wang, D., Gouhier, T. C., Menge, B. A., & Ganguly, A. R. (2015). Intensification and spatial homogenization of coastal upwelling under climate change. *Nature*, 518(7539), 390–394. <https://doi.org/10.1038/nature14235>

Supplement of

Intensified upwelling: normalized sea surface temperature trends expose climate change in coastal areas

Miguel Ángel Gutierrez-Guerra et al

Corresponding author: Miguel A. Gutierrez-Guerra, miguel.gutierrez104@alu.ulpgc.es

Supplementary:

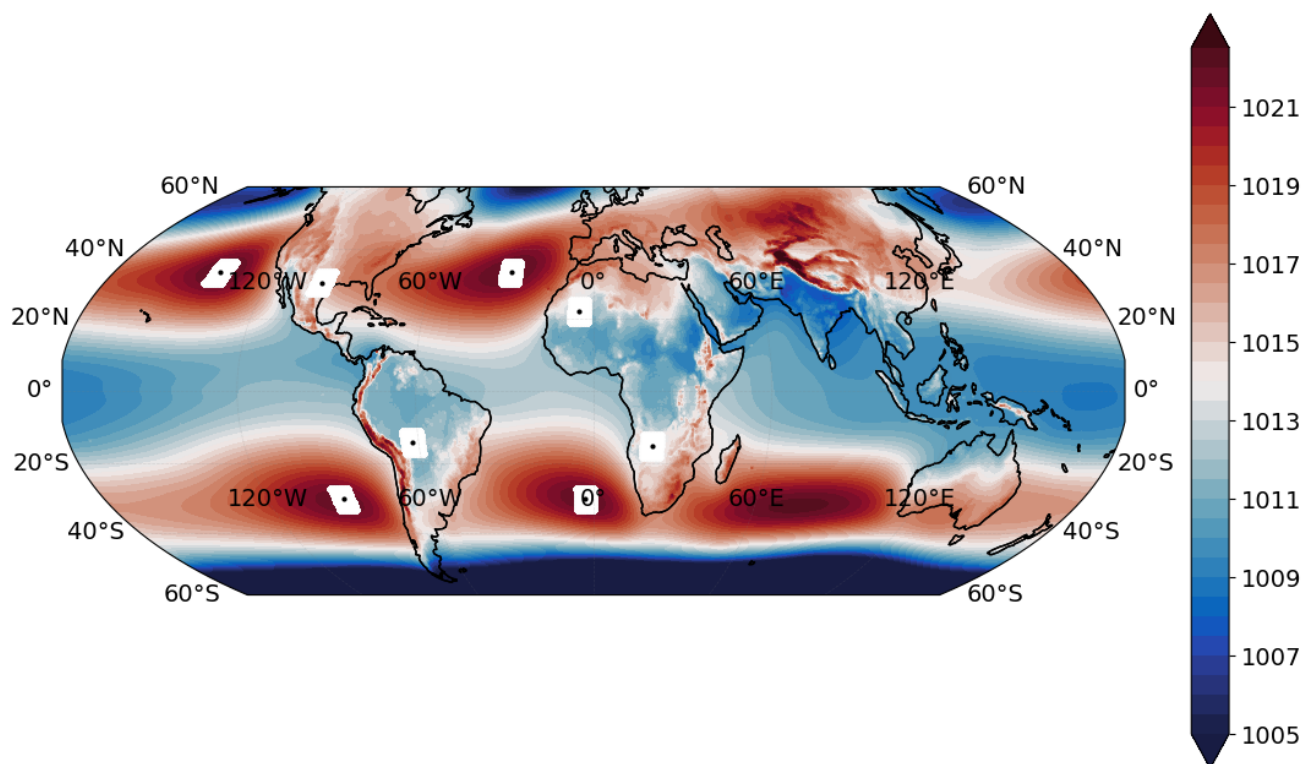
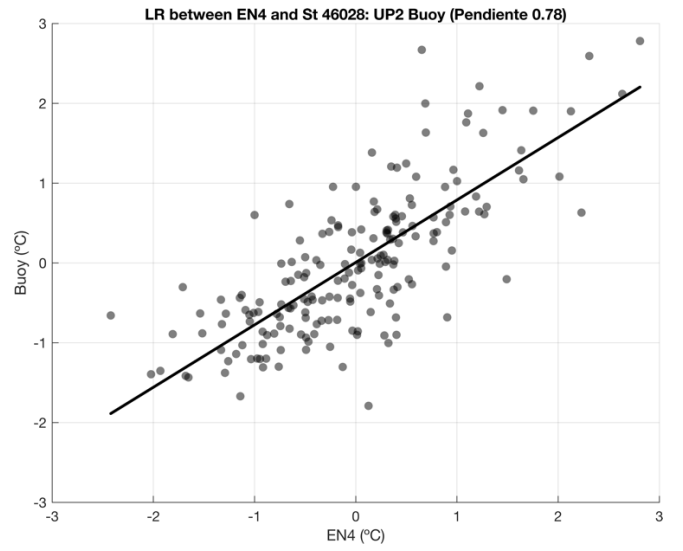
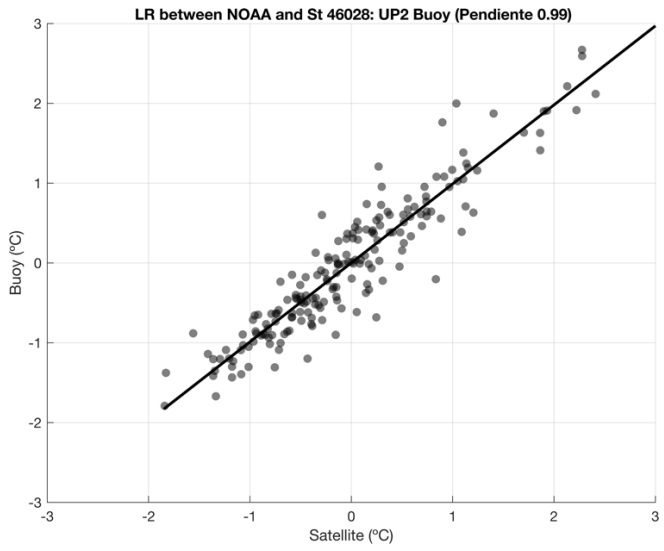
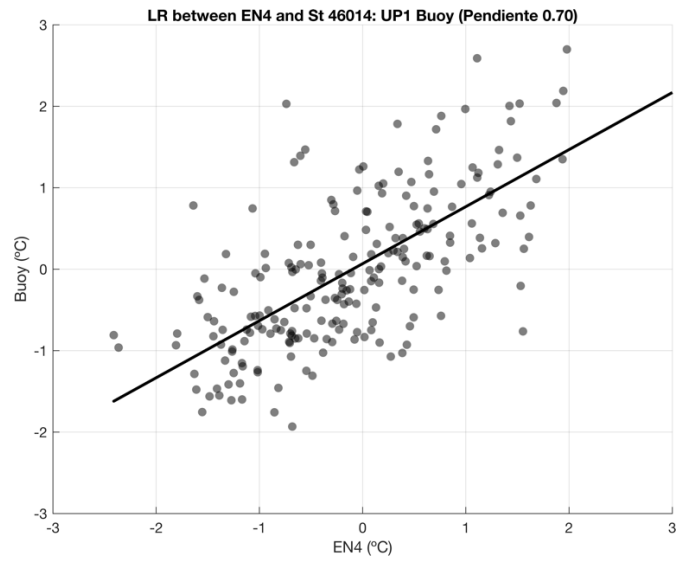
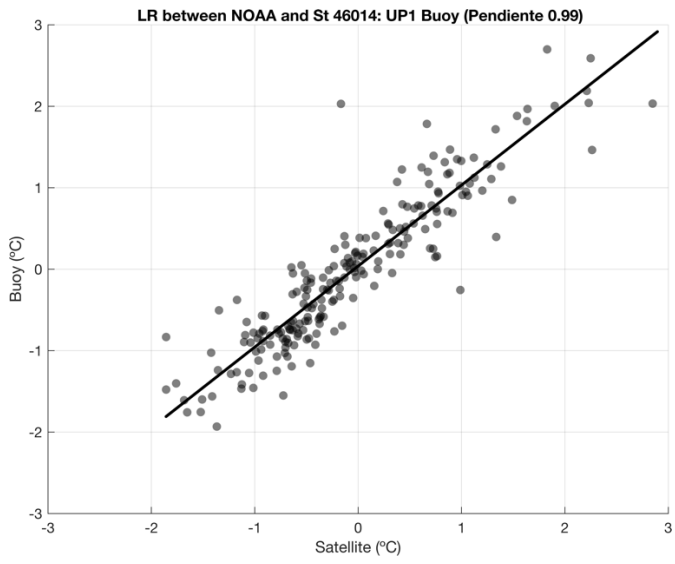
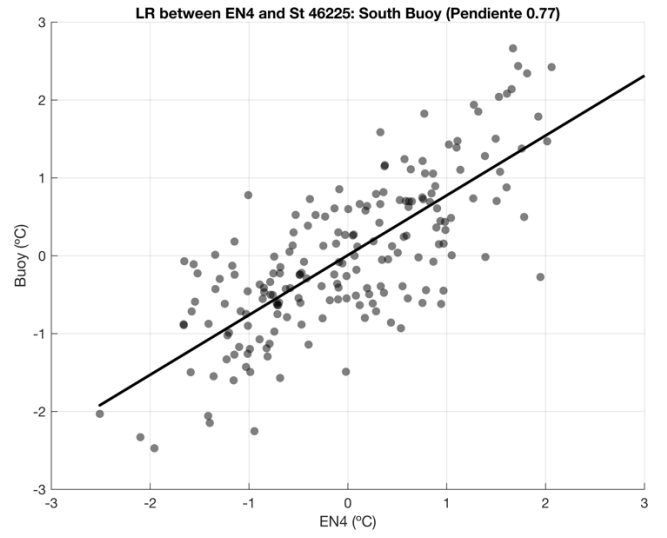
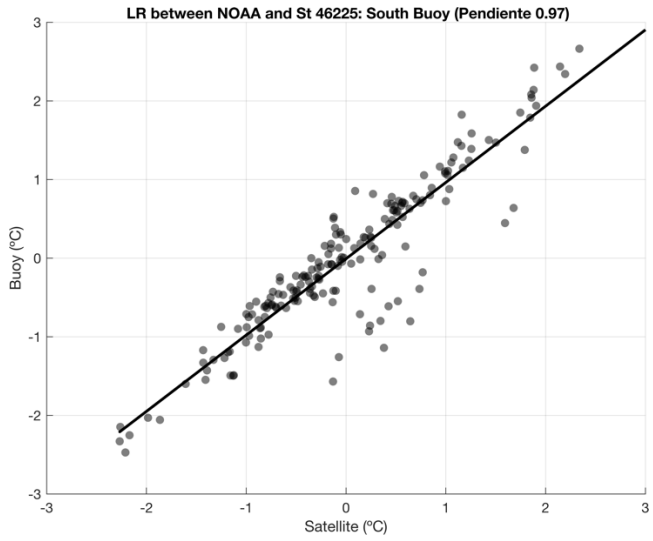
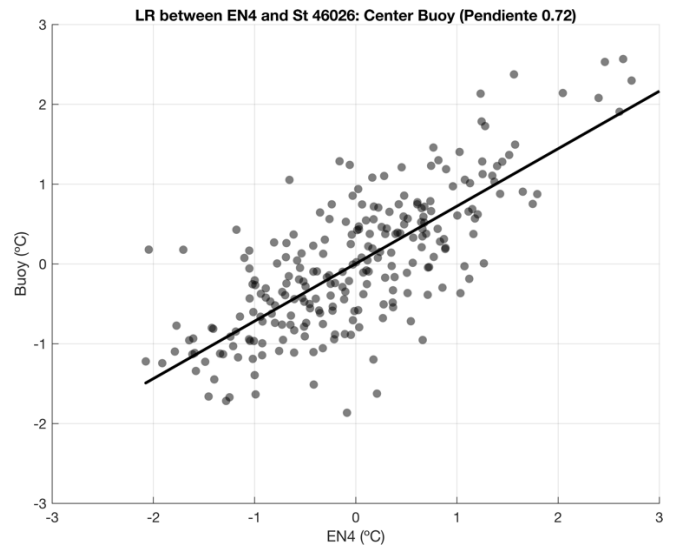
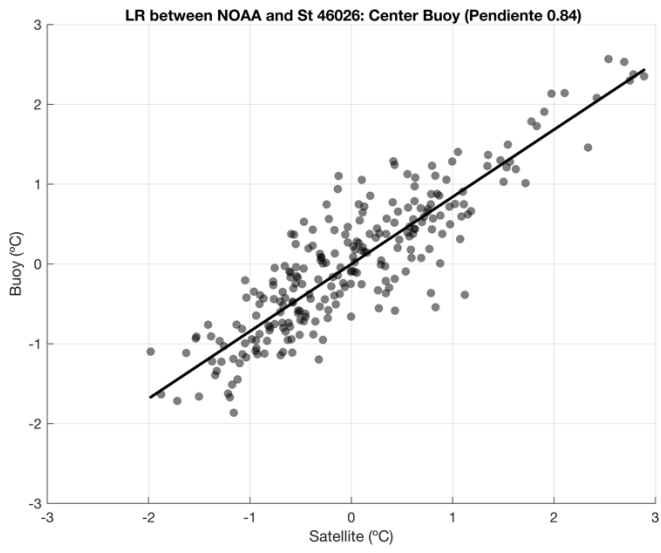


Fig S1: Mean field of SLP (1982-2023) from the ERA5 datasets. Black dots indicate the core of the pressure systems, while white points denote the area used for calculating the standard deviation





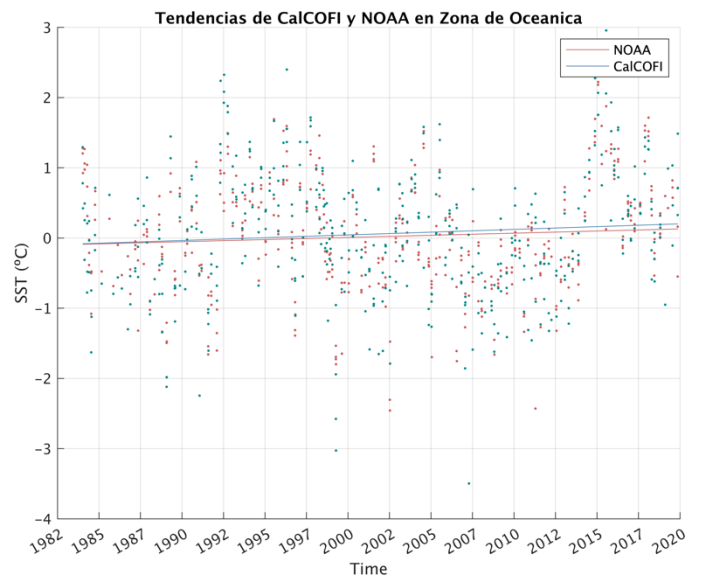
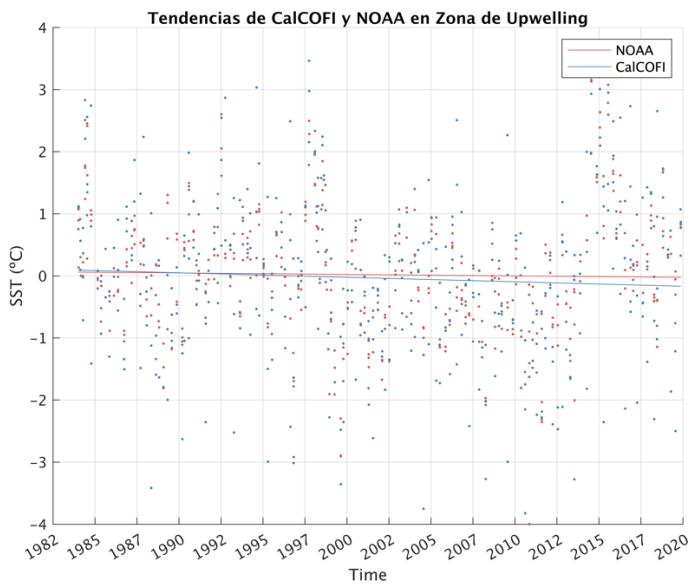
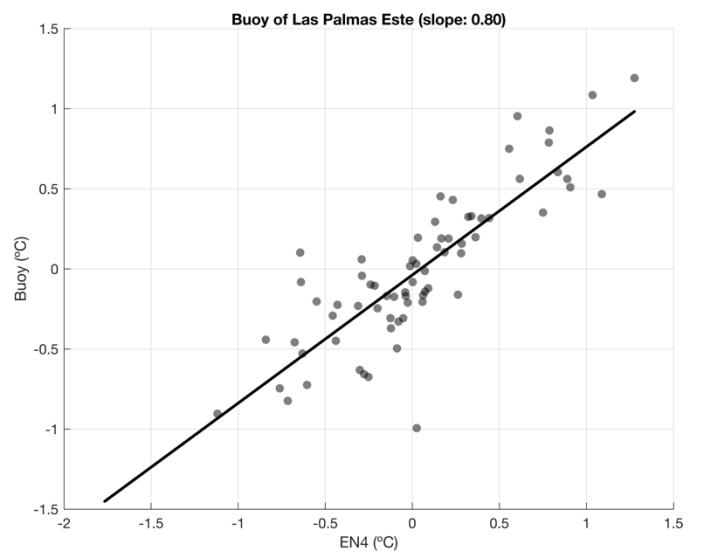
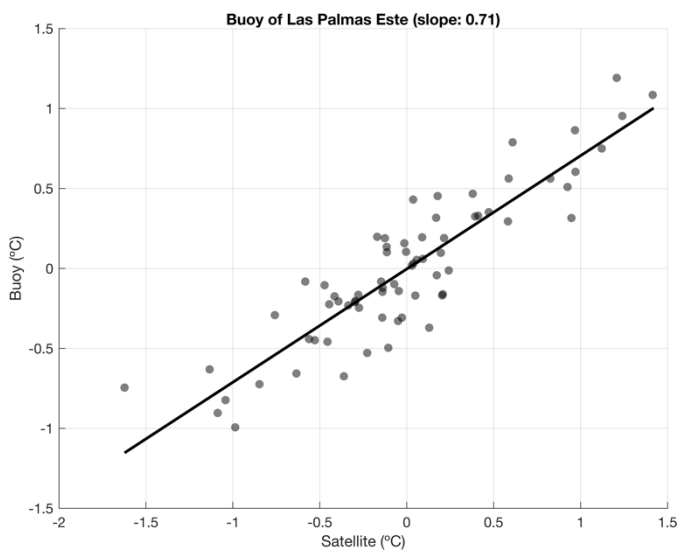
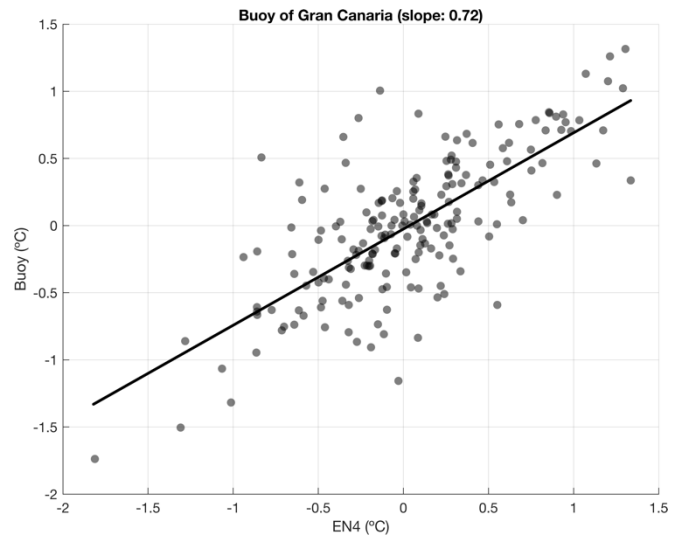
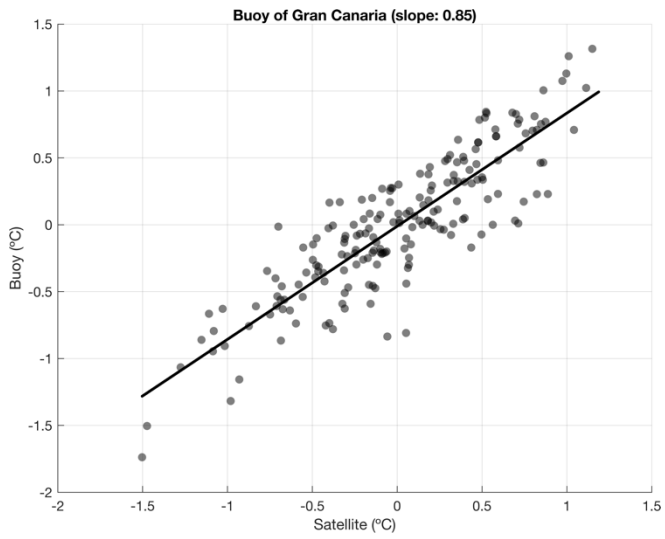
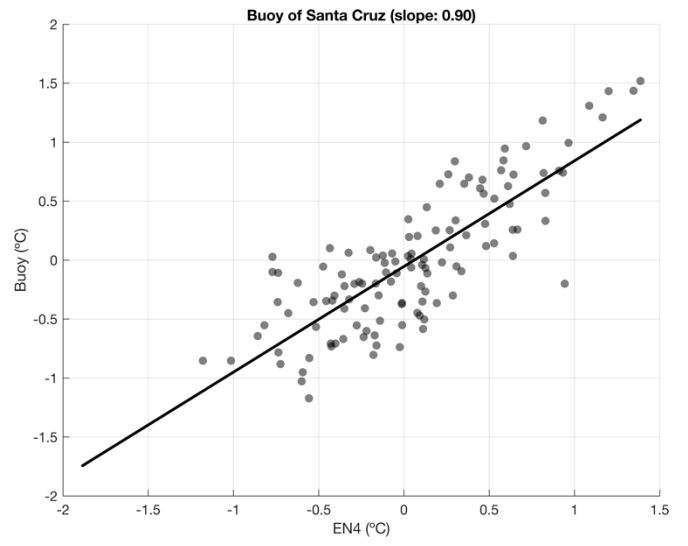
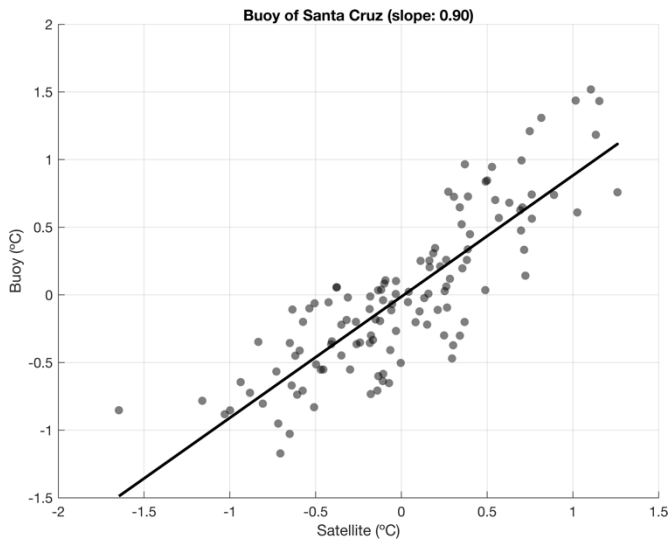


Fig S2: Validation of the reanalysis data with in-situ for the Pacific Ocean. This graphs complement Table 1.





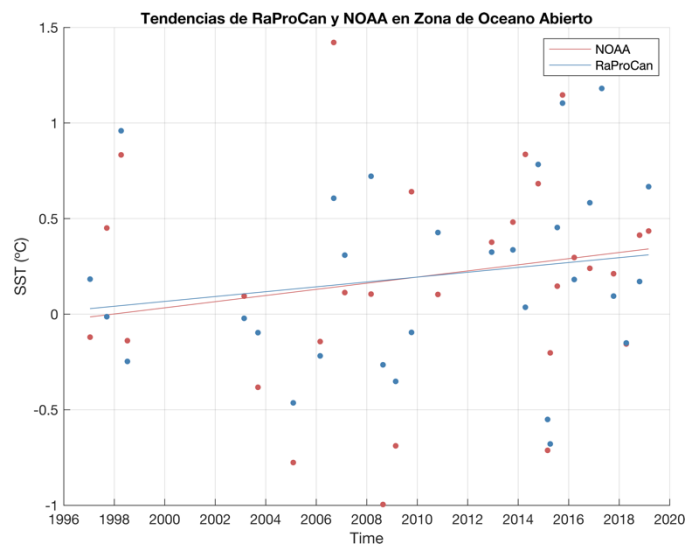
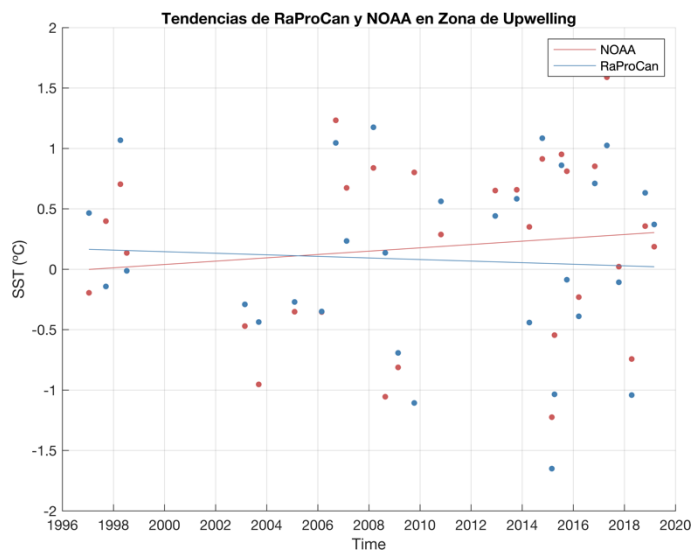
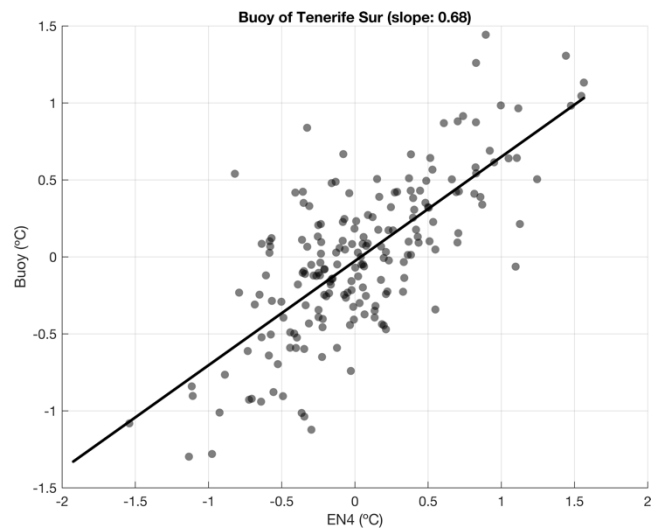
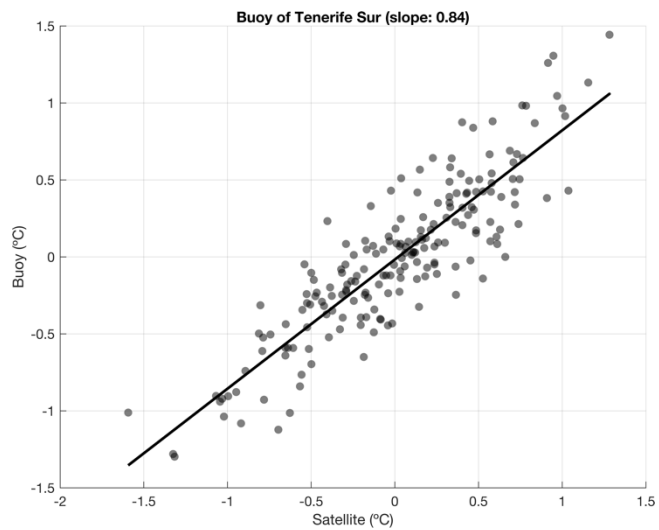
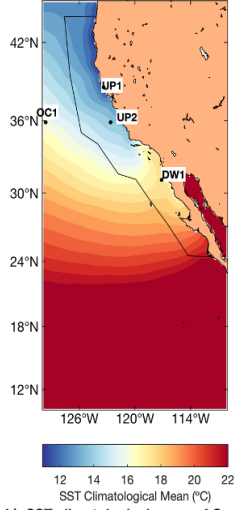
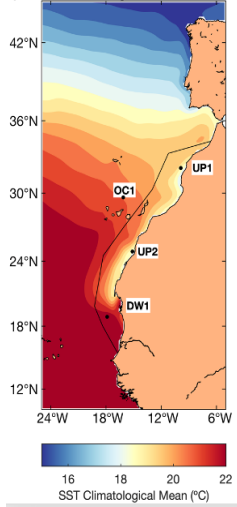


Fig S3: Validation of the reanalysis data with in-situ for the Atlantic Ocean. This graphs complement Table 2.

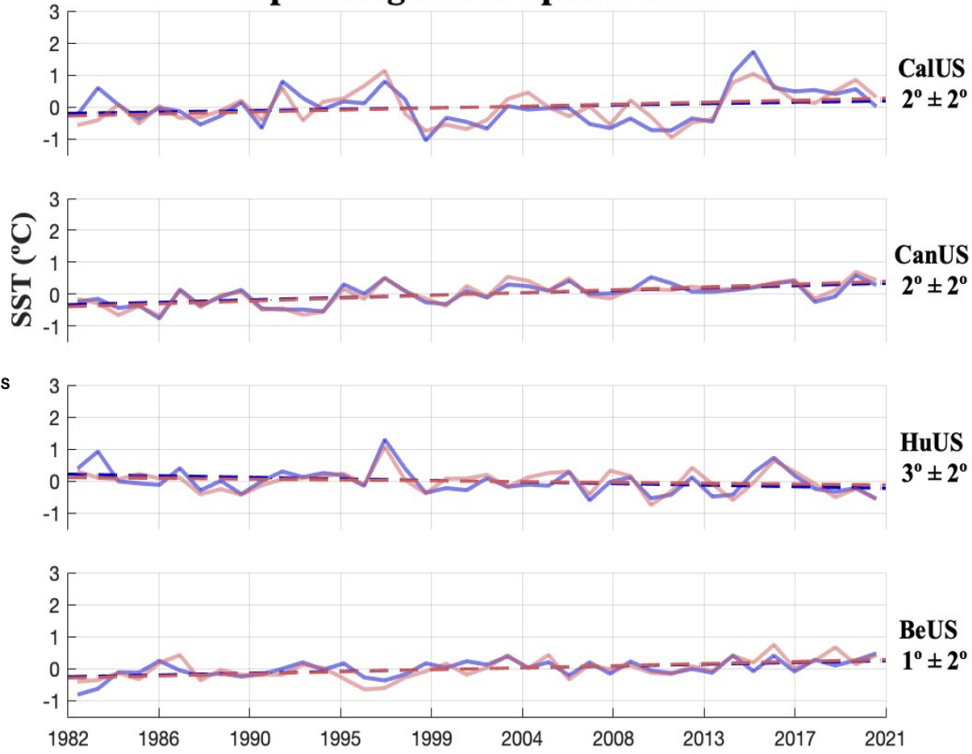
a) SST climatological mean of CalUS



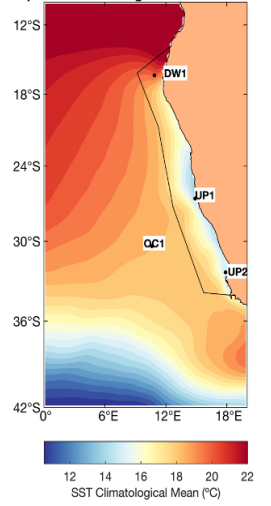
b) SST climatological mean of CanUS



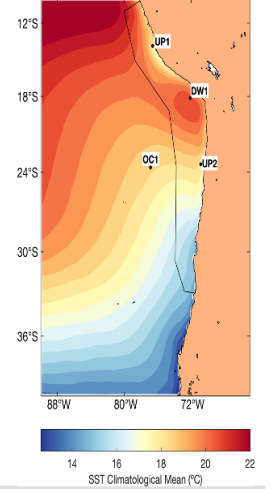
Upwelling cell vs open Ocean



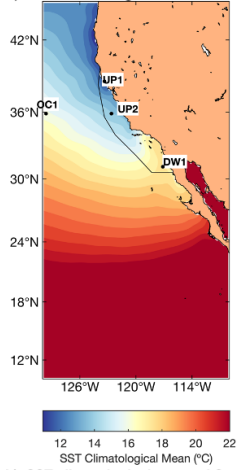
d) SST climatological mean of BeUS



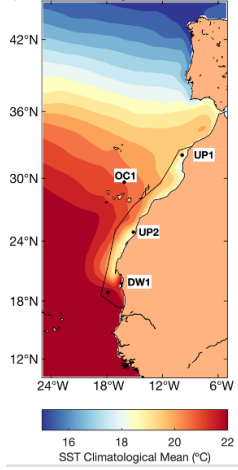
c) SST climatological mean of HuUS



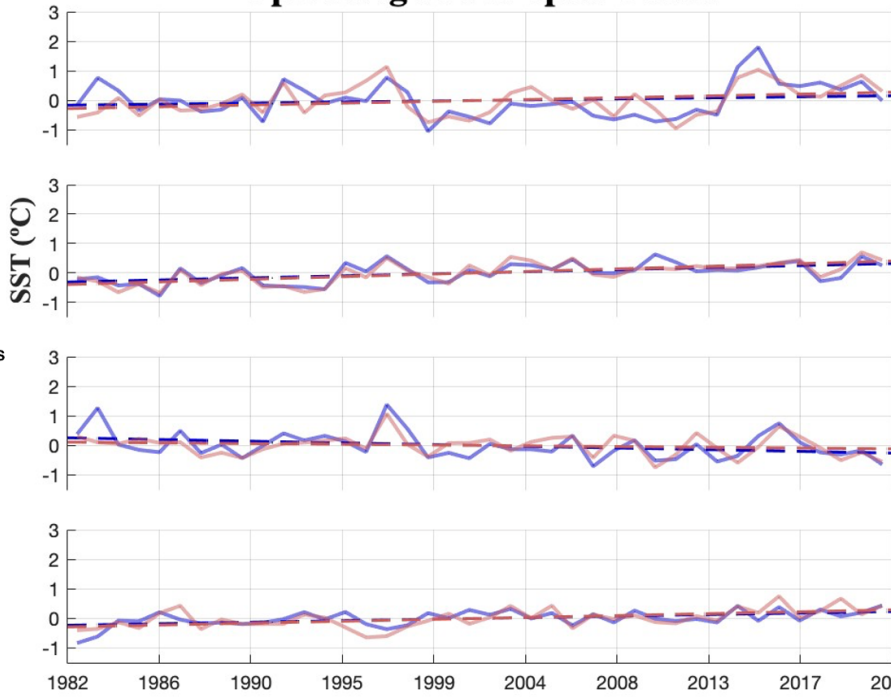
a) SST climatological mean of CalUS



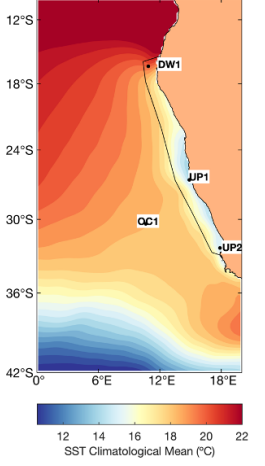
b) SST climatological mean of CanUS



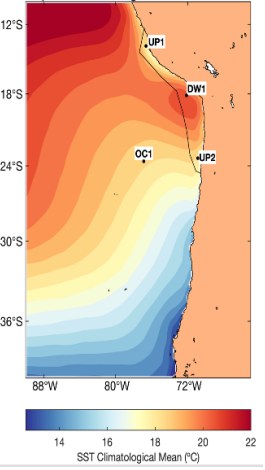
Upwelling cell vs open Ocean



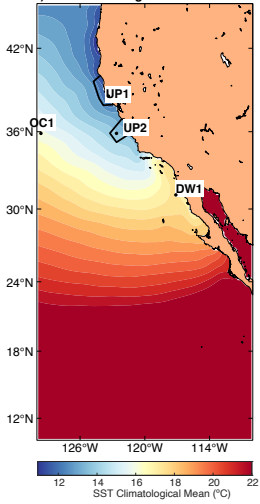
d) SST climatological mean of BeUS



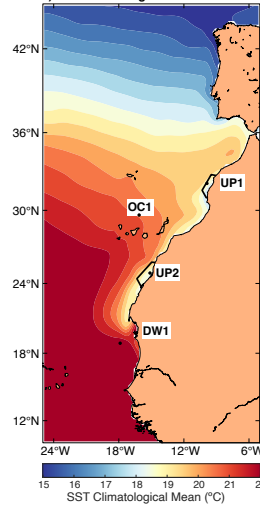
c) SST climatological mean of HuUS



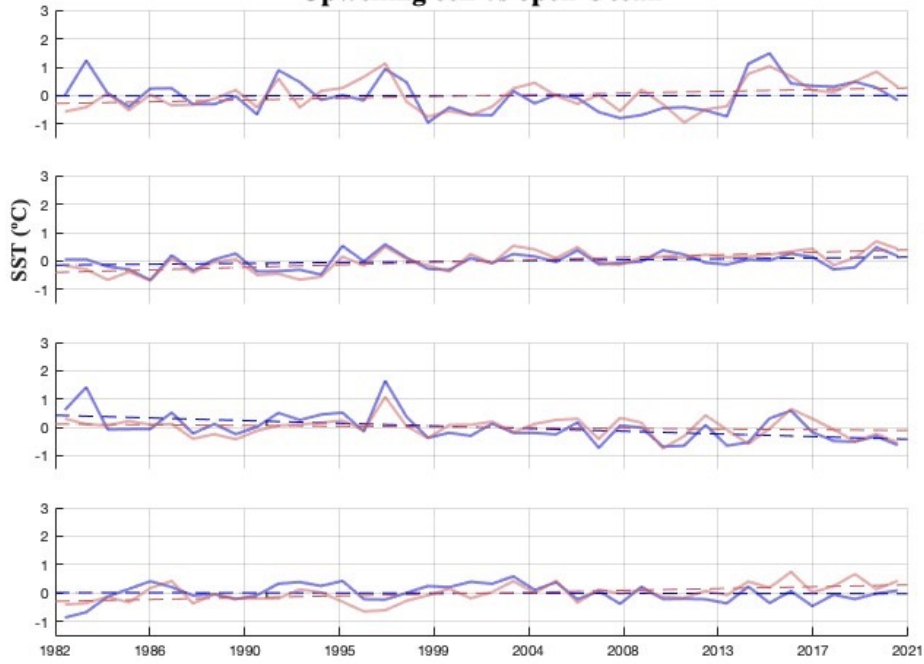
a) SST climatological mean of CalUS



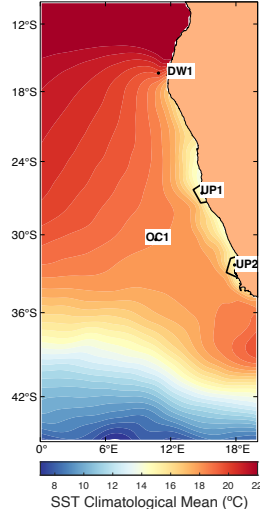
b) SST climatological mean of CanUS



Upwelling cell vs open Ocean



d) SST climatological mean of BeUS



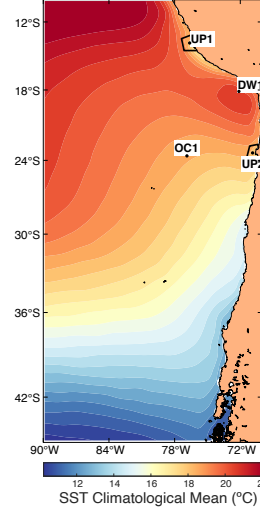
CalUS
 $8^\circ \pm 3^\circ$

CanUS
 $7^\circ \pm 2^\circ$

HuUS
 $9^\circ \pm 2^\circ$

BeUS
 $9^\circ \pm 2^\circ$

c) SST climatological mean of HuUS



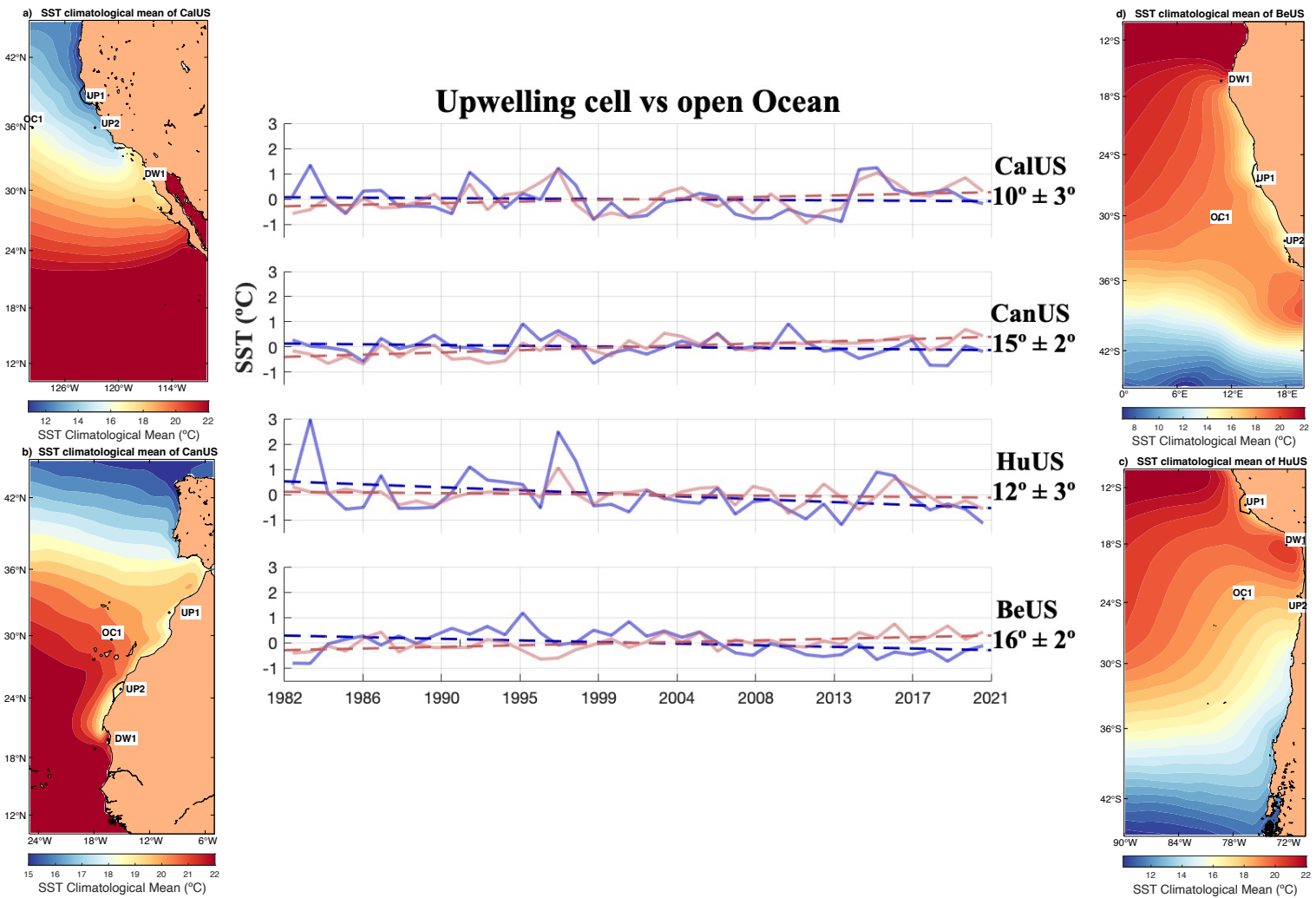


Fig S4: Same as Fig 5, but with α_{UI} recalculated for different averaged coastal regions (from Zone A at the top panel to Zone D at the bottom panel) compared to the OC1 point. The side maps display the averaged coastal areas outlined by black lines.

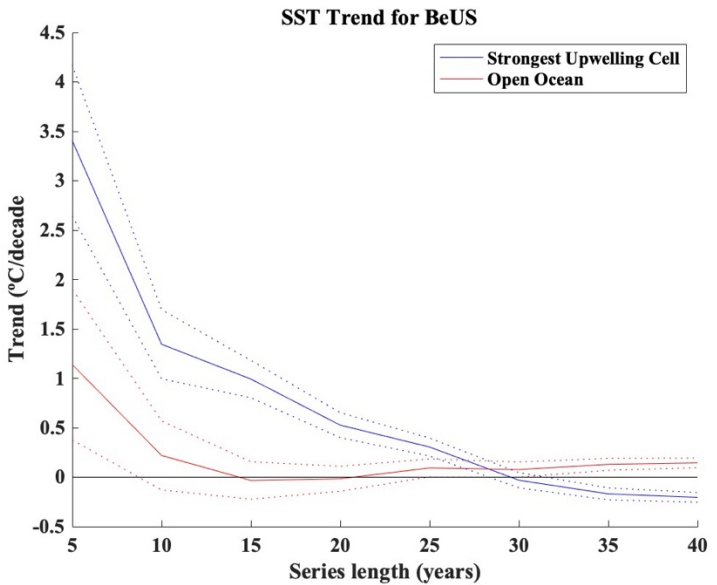
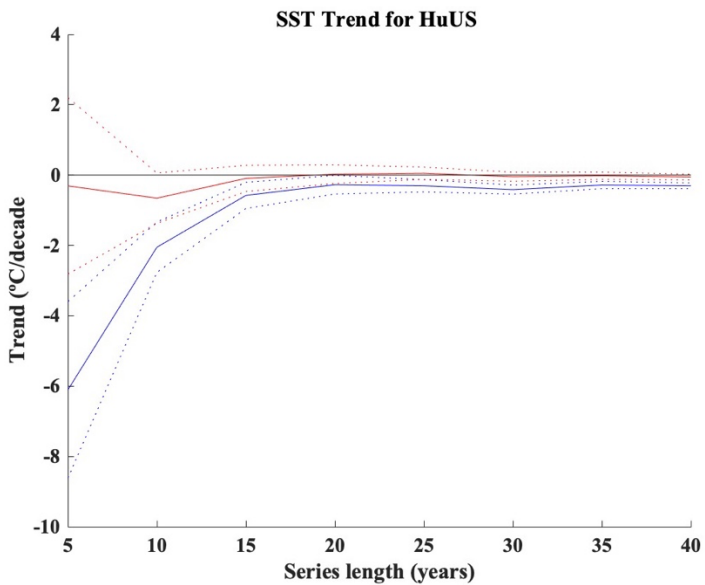
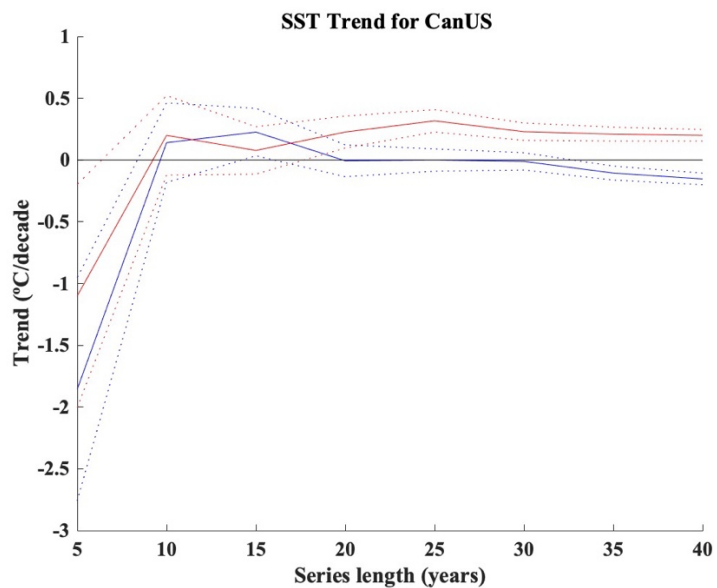
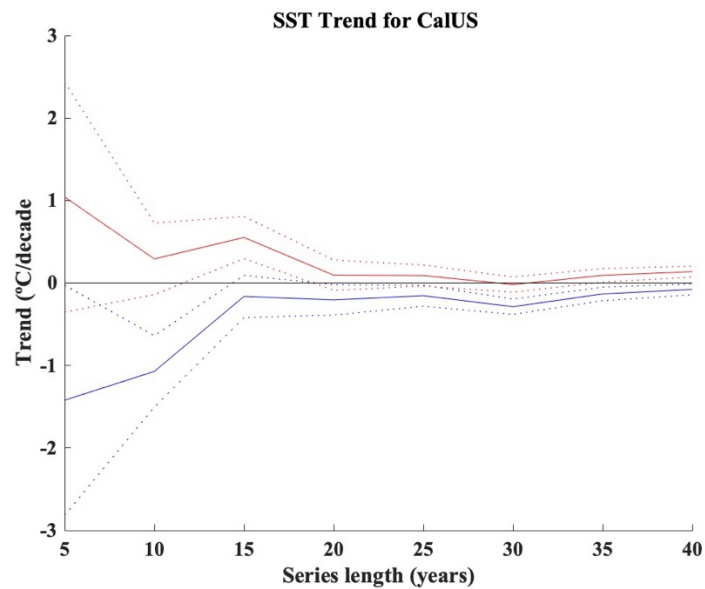


Fig S5: Trend values calculated as a function of series length for SST trends in the higher upwelling cell and open ocean areas. Trend values are shown as solid lines and 90% confidence limits as broken lines.

Zone	CalUS	CanUS	HuUS	BeUS
A	$2^{\circ} \pm 2^{\circ}$	$2^{\circ} \pm 2^{\circ}$	$3^{\circ} \pm 2^{\circ}$	$1^{\circ} \pm 2^{\circ}$
B	$3^{\circ} \pm 2^{\circ}$	$2^{\circ} \pm 2^{\circ}$	$4^{\circ} \pm 2^{\circ}$	$2^{\circ} \pm 2^{\circ}$
C	$8^{\circ} \pm 3^{\circ}$	$7^{\circ} \pm 2^{\circ}$	$9^{\circ} \pm 2^{\circ}$	$9^{\circ} \pm 2^{\circ}$
D	$10^{\circ} \pm 3^{\circ}$	$15^{\circ} \pm 2^{\circ}$	$12^{\circ} \pm 3^{\circ}$	$16^{\circ} \pm 2^{\circ}$
This Study	$11^{\circ} \pm 3^{\circ}$	$20^{\circ} \pm 2^{\circ}$	$14^{\circ} \pm 3^{\circ}$	$21^{\circ} \pm 2^{\circ}$

Table S1: α UI estimation for different portions of the coastal region: the whole coastal area, Zone A, covered an area just large enough to include the three main coastal upwelling areas (UP1, UP2 and DW1), Zone B, focused around the two main upwelling centers of each region, and Zone C, and targeted only the strongest upwelling center, Zone D. Last Row show the results obtained in Fig 5.